Nanoscale Res Lett (2008) 3:25–30
DOI 10.1007/s11671-007-9109-x

NANO EXPRESS

Excellent Field Emission Properties of Short Conical Carbon Nanotubes Prepared by Microwave Plasma Enhanced CVD Process

Sanjay Kumar Srivastava · Vasant D. Vankar · Vikram Kumar

Received: 15 November 2007 / Accepted: 22 November 2007 / Published online: 5 December 2007

Abstract Randomly oriented short and low density conical carbon nanotubes (CNTs) were prepared on Si substrates by tubular microwave plasma enhanced chemical vapor deposition process at relatively low temperature (350–550 °C) by judiciously controlling the microwave power and growth time in $C_2H_2 + NH_3$ gas composition and Fe catalyst. Both length as well as density of the CNTs increased with increasing microwave power. CNTs consisted of regular conical compartments stacked in such a way that their outer diameter remained constant. Majority of the nanotubes had a sharp conical tip (5–20 nm) while its other side was either open or had a cone/pear-shaped catalyst particle. The CNTs were highly crystalline and had many open edges on the outer surface, particularly near the joints of the two compartments. These films showed excellent field emission characteristics. The best emission was observed for a medium density film with the lowest turn-on and threshold fields of 1.0 and 2.10 V/μm, respectively. It is suggested that not only CNT tip but open edges on the body also act as active emission sites in the randomly oriented geometry of such periodic structures.

Keywords Carbon nanotubes · CVD · Microwave plasma CVD · Field emission · Conical CNTs

S. K. Srivastava (✉) · V. Kumar
Electronic Materials Division, National Physical Laboratory, Dr. K.S. Krishnan Marg, Pusa, New Delhi 110012, India
e-mail: srivassk@mail.nplindia.ernet.in

V. D. Vankar
Department of Physics, Thin Film Laboratory, Indian Institute of Technology Delhi, Hauz Khas, New Delhi 110016, India

Introduction

Carbon nanotubes (CNTs) [1] have attracted wide attention both in the research and industrial communities because of their unique structure and properties. In particular, field electron emission from CNTs has been proposed to be one of the most promising as far as its practical application is concerned. This is because CNTs present many advantages over conventional Spindt (Mo, Si, etc.) emitters [2] such as (i) high chemical stability (resistance to oxidation or other chemical species) and high mechanical strength (Young's modulus $\sim$1 TPa), (ii) high melting point ($\sim$3,550 °C) and reasonable conductivity (resistivity $\sim 10^{-7}$ Ωm), (iii) high aspect ratio (>1,000) with very small tip radius to greatly enhance the local electric field, and (iv) easy and low cost production [3].

The potential of CNTs for field emission (FE) was first reported in 1995. FE from an isolated single multiwalled CNT (MWNT) was first observed by Rinzler et al. [4] and that from a MWNT film was reported by de Heer et al. [5]. Since then a number of experimental studies on FE aspects of both MWNTs [6–16] and single-walled CNTs [17, 18] grown by different processes such as arc discharge and various versions of chemical vapor deposition (CVD) both with and without plasma have been investigated. Many parameters such as density, length of CNTs, spacing between neighboring nanotubes, open/closed tips, presence of adsorbates, metal particles, etc., have been reported to affect the FE characteristics of CNT films. Carbon nanostructures other than CNTs, such as carbon nanofibers (CNFs) [19, 20], carbon nanocones (CNCs) [21, 22], carbon nanosheets/nanowalls [23, 24], etc., are also promising material structure as field emitters. Recently, there have been continuous efforts on growth of one-dimensional carbon nanostructures with a very sharp tip structure

because it can enhance the FE characteristics significantly [25–28]. Low density of such structures is indispensable for FE due to the screening effect [11–15]. There have been few studies on the role of length, density/spacing between CNTs on the FE characteristics of CNT films [12–15]. However, most of them are for the vertically aligned CNTs and there are very limited related investigations on the randomly oriented CNTs [10, 11]. The structural characteristic of the CNTs is critical for FE and is not discussed in any of the above reports. This is important because CNTs prepared by low temperature plasma CVD process have many structural defects. For example, CNTs prepared by PECVD process using any hydrocarbon and NH_3 or N_2 generally have bamboo-structure popularly known as bamboo-shaped CNTs (BS-CNTs) [29–31]. Hence the motivation of the present study was to grow CNTs films of varying density and length and co-relate their structural and FE characteristics.

In this article, films having randomly oriented short and cone-shaped CNTs have been grown on Si substrates by tubular MPECVD process at relatively low temperature through judicious control over the process parameters such as microwave power and growth time. Iron (Fe) thin films deposited on Si substrates were used as the catalyst. Acetylene (C_2H_2) and NH_3 were used as feed and dilution gases, respectively. The field emission measurements showed that they had excellent emission characteristics compared to long and high-density BS-CNT films. It is suggested that not only nanotube tips but open edges on the body also act as active emission sites in the randomly oriented geometry of these structures giving enhanced emission characteristics.

Experimental

Carbon films were deposited by tubular MPECVD process on p-Si (100) substrates. The details of the experimental set up is described elsewhere [23]. In brief, tubular MPECVD system is equipped with a 1.2 kW, 2.45 GHz microwave source and a traverse rectangular wave-guide to couple the microwave to a tubular quartz tube for generating the plasma. No additional heater was used for substrate heating. It was heated directly by the plasma. The substrate was placed on a quartz holder that was fully electrically insulated and the substrate was fully immersed in the plasma zone. No additional substrate biasing of the substrate was made. Thin films of Fe $\sim$10 nm were deposited on chemically cleaned Si wafers by thermal evaporation technique at a base pressure of 2.0×10^{-6} Torr and no buffer layer was used between Fe film and Si substrates. Fe-coated Si substrates were then loaded into the reactor chamber for growth process. Growth process includes the two steps: (i) pretreatment of Fe film in NH_3 plasma followed by (ii) introduction of C_2H_2 for carbon film deposition. The pretreatment of Fe films had three main objectives: (i) heating the substrate to the desired growth temperature, (ii) etching of Fe film by active plasma species, and (iii) conversion of the Fe film into Fe nanoparticles needed for CNTs nucleation and growth. The Fe films were pretreated in NH_3 plasma for 10 min at input microwave powers of 300–450 W, operating pressure of 5 Torr and with NH_3 flow rate of 40 sccm. CNT films were deposited at different microwave power varying from 300 to 450 W for a fixed C_2H_2/NH_3 flow rate ratio of 20/40 and a pressure of 5 Torr for 3 min. Under these conditions, substrate temperature varied in the range of 350–550 °C.

Scanning electron microscope (SEM) (LEO 435 VP) operating at 15 kV was used for surface morphological features of the films. Transmission electron microscope (TEM) (Philips, CM 12) operating at 100 kV and high-resolution TEM (HRTEM) (TECNAI 20UT) was used for structural analysis of CNTs. The process of TEM specimen preparation is described in our previous article [29]. Field emission measurements were carried by planar diode assembly at a base pressure of $\sim 2.0 \times 10^{-6}$ Torr [23]. Spacing between electrodes (d) was kept $\sim$300 μm. FE current was measured with increasing voltage. Emission current density was calculated by dividing the emission current with the exposed area of the sample [32].

Results and Discussion

Figure 1 shows the SEM micrographs of samples deposited at microwave power of 300, 350, 400, and 450 W (named as sample 1, sample 2, sample 3, and sample 4, respectively). It is clearly seen that no nanotube is observed for sample 1 (Fig. 1a) and highly magnified image as shown in the inset shows that nanotubes remain in their nucleation stage. Very short length and low density of nanotubes is observed in sample 2 (Fig. 1b). However, for samples 3 and 4, density and length increased significantly as shown in Fig. 1c and d, respectively. Almost 50% of the area is covered by CNTs and rest is covered by either catalytic nanoparticles (bright contrast) or very short nanotubes. In case of sample 4, almost whole area is covered with nanotubes. The length and density of the CNTs estimated by SEM study for these samples are given in Table 1. Both the length and density of CNTs increased with increasing microwave power. It is clear that large density of catalytic nanoparticles is formed after NH_3 plasma pretreatment. These catalytic particles seed the nucleation and growth of nanotubes after C_2H_2 introduction in the plasma. Each nanotube has a catalyst nanoparticle mostly in the base region, which clearly indicates that the growth is catalytic.

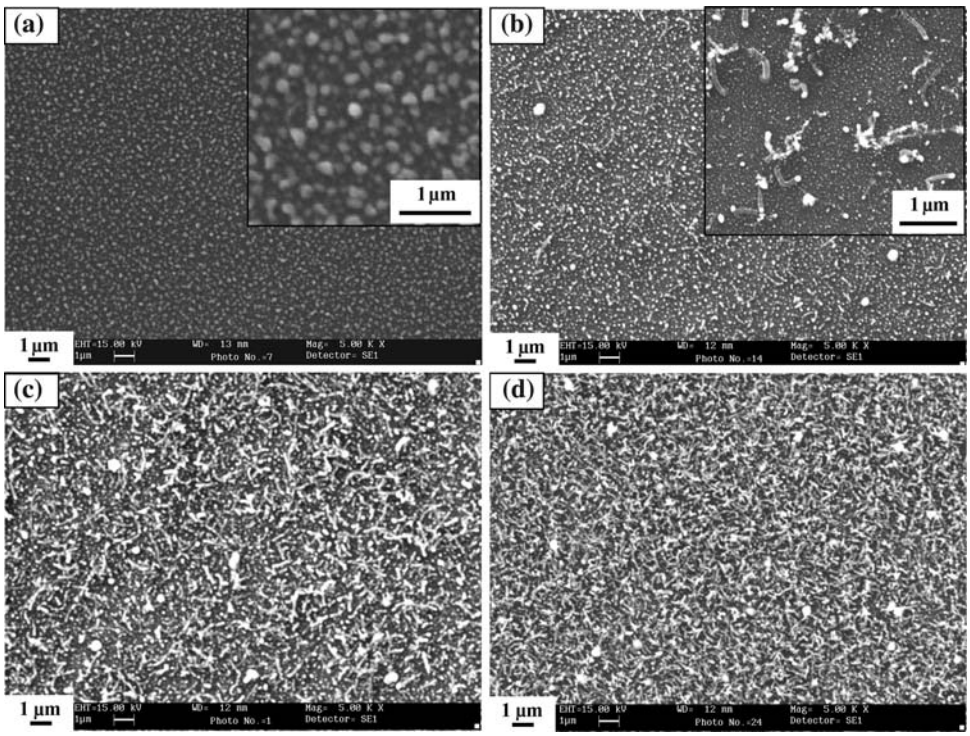

Fig. 1 SEM micrographs of CNT samples deposited at different microwave power (**a**) sample 1, (**b**) sample 2, (**c**) sample 3, and (**d**) sample 4. The magnified views of (**a**) and (**b**) are shown in the respective insets

Table 1 Comparison of microstructural features (such as length, density) and field emission parameters (E_{to}, E_{th}, and β) of samples 2, 3, and 4

Sample	Length (μm)	Density ($\times 10^7$ cm^{-2})	E_{to} (V/μm)	E_{th} (V/μm)	β
2	0.5–0.8	~6	2.67	–	2528
3	0.5–1.5	~20	1.60	2.75	6953
4	1.5–3.0	~35	1.00	2.10	15724

Note: E_{to} is the macroscopic field required for emission current density of 10 μA/cm^2, and E_{th} is the field for emission current density of 1 mA/cm^2

CNTs have generally conical shape as one shown in the inset of Fig. 1b. At low microwave power, the plasma density is low and hence slow rate of carbon supply to the catalyst particles is expected. The substrate temperature is also low since it is plasma dependent in the present geometry and hence slow growth rate. Consequently, very short length and low density CNTs are observed at low input microwave power. With increase in microwave power both plasma density and substrate temperature increase, resulting more number of CNTs nucleation and growth. CNTs of varying length are observed due to different catalyst particle sizes [33].

These samples were examined by TEM for determination of length, diameter, and internal structure of CNTs. Representative TEM micrograph of the short length CNTs is shown in Fig. 2a. It is clearly seen that CNTs consist of regular and very short conical compartments stacked over each other. The maximum length of CNTs was observed to be ~3 μm and the shortest nanotube observed by TEM was ~500 nm. The outer diameter of these nanotubes varied in the range of 30–70 nm. It is to be noticed that these short CNTs have very sharp tips of diameter in the range of 5–20 nm. In general, tip diameter was estimated to be approximately one-fourth of the outer diameter of the tube body. Representative TEM micrograph showing full-length view of such very short conical nanotube is shown in Fig. 2b. The highly magnified view of nanotube tip is shown in Fig. 2c. Clearly the wall thickness in the tip compartment is very less compared to that in the preceding compartments. The wall thickness is the maximum at the joint of two compartments and it decreases gradually toward the middle of a particular compartment and continues till the beginning of the next compartment. Each compartment is of an almost equal length except the tip one. The conical compartments are stacked in such a way that total outer diameter of the tube body remains almost constant. The other side of the tube is either open or has a cone/pear-shaped catalytic particle (Fig. 2a, b). This side is definitely the base of the conical CNTs. Therefore, the growth of short conical CNTs in present study is governed by the base growth mode [34]. The short CNTs are highly crystalline as observed by HRTEM micrograph shown in Fig. 2d. Compartments consist of parallel planes with an inter-planar spacing of ~0.34 nm. Because of the conical shape, these walls are inclined toward the tube axis making an acute angle of ~5–6° in general. However, in some

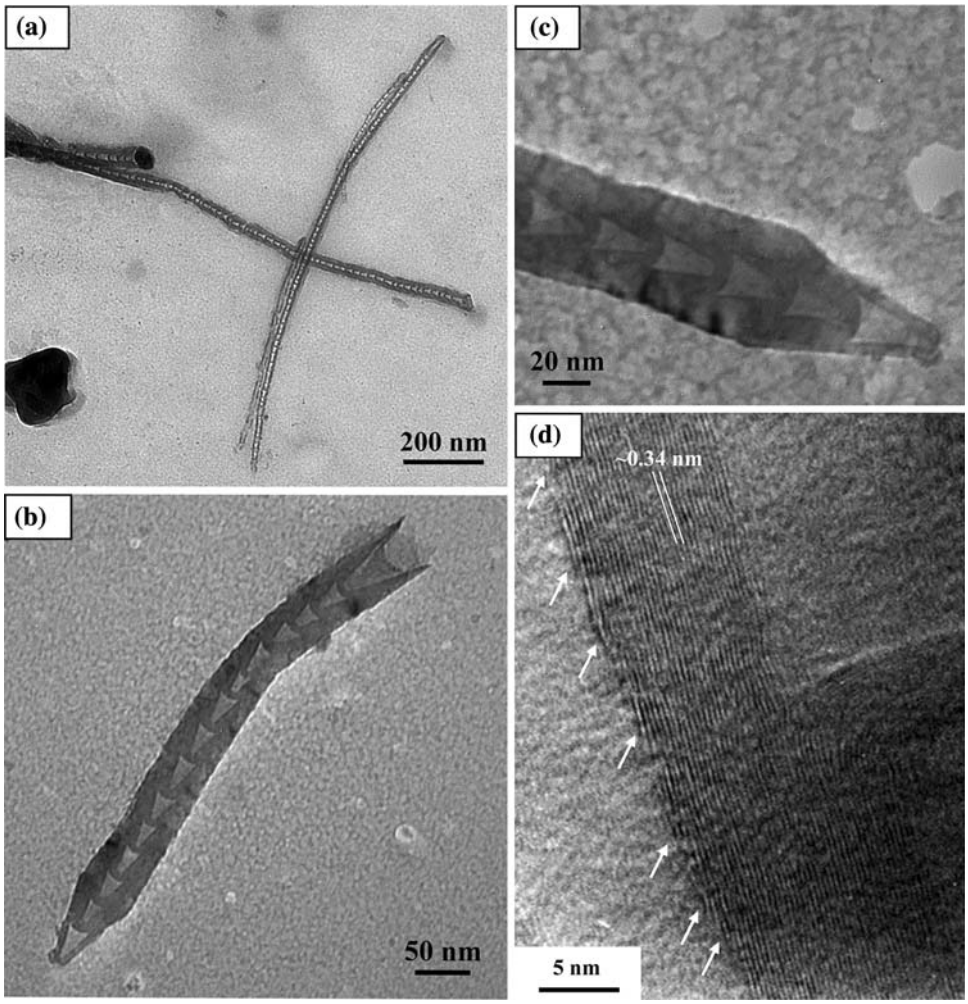

Fig. 2 TEM micrographs of short conical CNTs (**a**) low magnification image, (**b**) magnified view of the shortest conical CNTs, (**c**) highly magnified view of tip, and (**d**) typical HRTEM image of a conical CNT

tubes this angle was observed to be $\sim 10°$. Clearly, the number of walls is maximum at the joint of two compartments and minimum near the middle of the compartment. It is to be noticed that there are many open edges on the outer surface of the tube as indicated by arrows in Fig 2d. This is attributed to their periodic structure and the stacking arrangement of constituent compartment walls.

The growth mechanism of such periodic structure with a sharp conical tip has been discussed in our previous article [29], where it is suggested that nitrogen and atomic hydrogen plays a significant role in the formation of compartmentalized structure. It is shown by in situ optical emission spectroscopy that high concentration of CN and H species present in the $NH_3 + C_2H_2$ plasma facilitate the growth of BS-CNTs [29]. The periodic appearance of conical structure in one tube is supposed to be due to periodic precipitation of the graphite sheets on the top surface of the catalyst particle under steady state. The catalyst particles were in quasi-liquid state during growth and the high surface energy of the precipitating graphite layers moulded the particles to acquire the stable minimum energy configuration and hence the conical shape. The growth of highly crystalline CNTs at relatively low temperature could be due to high-density plasma. The plasma not only ionizes the gas but also causes a local surface heating [35]. Consequently, by this method growth temperature could be greatly decreased compared to other non-plasma CVD processes. In addition, a small concentration of nitrogen doping is also reported in the compartmentalized CNT films [32]. It is also suggested that dangling bonds in the open edges of such periodic structure may be terminated by atomic hydrogen [36, 37].

Figure 3a shows the comparative emission current density (J) vs. macroscopic field (E) of samples 2, 3, and 4. No significant emission current was observed from sample 1. The emission measurements were carried out for two cycles with increasing and decreasing fields. Repeatable emission data were observed during both the cycles for the three samples. The comparative FE parameters such as turn-on (E_{to}) and threshold (E_{th}) fields of these samples are given in Table 1. This shows that emission performance improves with increasing CNTs density and length. Sample

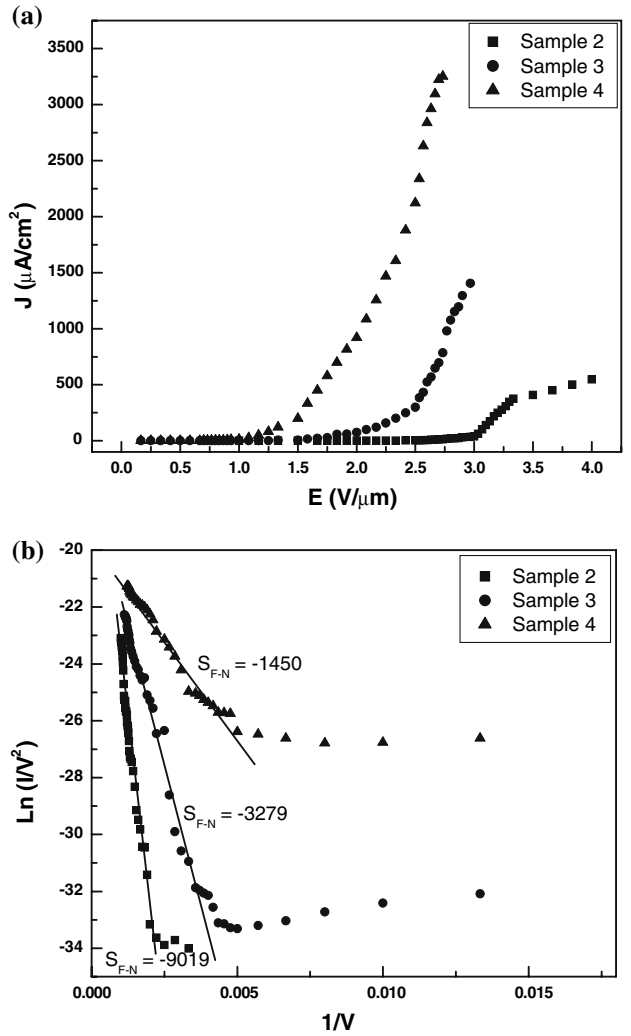

Fig. 3 (**a**) Emission current density (*J*) vs. macroscopic electric field (E) of samples 2, 3, and 4. (**b**) F–N plots of sample 2, sample 3, and sample 4

4 has the lowest E_{to} and E_{th} values. This is because number of emission sites increases with increasing both length and density of CNTs. However, very high density ($>10^9$ cm^{-2}) and longer ($\sim$10–15 μm) randomly oriented or vertically aligned CNT (with similar structure) films had poor emission characteristics than that of sample 4 [32], which could be due to screening effect. This suggests that sample 4 has the optimum combination of length and density of conical periodic structured CNTs in random orientation configuration for the best emission.

Field emission is usually analyzed using Fowler–Nordheim (F–N) theory, according to which emission current density is dependent on the local electric field (E_{loc}) and chemical state (i.e. work function, ϕ) of the emitter tip as $J \propto (E^2_{loc}/\phi)\ \exp(-B\phi^{3/2}/E_{loc})$ where $B = 6.83 \times 10^9$ VeV$^{-3/2}$ m^{-1}. The local field E_{loc} is related to the macroscopic field (E) by geometrical enhancement factor (β) as $E_{loc} = \beta E$. The β can be determined experimentally from the slope (S_{F-N}) of ln(I/V^2) vs. 1/V plot as $\beta = -B\phi^{3/2} d/S_{F-N}$, provided ϕ is known. In case of CNT films, emission occurs from multiple emitters and an integrated current is measured. There could be lot of variations in local fields due to various geometries of the emitters. Also, work function of each emitter is not necessarily same. This makes the exact analysis of field emission characteristics of CNT films difficult.

The F–N plots for the three samples are given in Fig. 3b. Interestingly single slope behavior is observed for all the samples in contrast to our high-density BS-CNTs films [32]. This is attributed to their lower density, which overcomes the field screening effect and interaction among neighboring CNTs [11, 14]. The geometrical enhancement factors determined from slopes of the F–N plots assuming $\phi = 5$ eV, are given Table 1. These are 2,528, 6,953, and 15,724 for samples 2, 3, and 4, respectively. Such a high field enhancement factor is accounted for the sharp tip and open edges on the surface of CNTs [9, 17]. In this calculation, the ϕ of CNTs is assumed as a constant, which is known to be strongly dependent on several factors such as structure/defects (e.g. capped, open, presence of metal particles, etc.) of CNTs [38], and surface states. As an example nitrogen incorporated in CNTs significantly reduces the work function [39] and hydrogen saturated surface (open edges terminated by hydrogen atoms) have much lower values than that of graphite ($\sim$5 eV) [40]. The exact experimental measurement of the work function for CNTs, especially in film form, is complicated [41]. Therefore, the enhancement factor determined by F–N plots is not truly correct and yields relatively higher values [39]. Hence, the enhanced FE characteristics of short conical CNT films should be attributed to the following: (i) an optimum length and density combination to overcome screening effect, (ii) sharp closed tips, and (iii) open edges on the outer surface of CNTs which enhance the local field. These open edges also act as additional emission sites [42]. In addition, other favorable conditions for enhanced emission of such periodic structured conical CNTs could be: (a) N doping in CNTs, which can increase the local density of states near the Fermi level [43], (b) hydrogen saturation of open edges on the surface which also decrease the effective work function. It is also important to note that no significant emission current was observed from sample 1 in the measurement range. This confirmed that the catalytic particles lying on the substrate had no contribution and emission occurred from CNTs only.

The field emission stability was also tested as in case of high density BS-CNTs [32]. These films also showed stable emission current with an average fluctuation of $\sim$2% and small decrease of $\sim$2% emission current was observed for sample 4 after continuous operation of 20 h. No significant

change in the morphology of the films was observed after such emission performance tests.

Conclusions

Films containing randomly oriented conical CNTs with varying length and density were grown on Si substrates by MPECVD process at relatively low temperature by judicious control of the process parameters such as microwave power and growth time. The CNTs have periodic compartmentalized structure with a sharp conical tip and many open edges on the body. These films have superior emission characteristics compared to high density vertically aligned or randomly oriented BS-CNT films. Lower density, sharp tips, defective body structure, and random orientation of CNTs have been suggested for the enhanced emission performance of these samples. It is known that there is a strong correlation between the density and length of aligned CNTs, where emission dominantly occurs from the tip region, for stable and high emission current density at low fields. However, for periodic structures like this, where emission can also occur from the body regions, controlling their length, density, and structure with the help of growth parameters would be very useful for field emission perspectives.

Acknowledgments One of the authors (S. K. Srivastava) is thankful to Dr. D. V. Sridhar Rao, DMRL, Hyderabad, for his assistance in HRTEM analysis of the samples.

References

1. S. Iijima, Nature **354**, 56 (1991)
2. C.A. Spindt, J. Appl. Phys. **39**, 3504 (1968)
3. P. Gröning, L. Nilsson, P. Ruffieux, R. Clergereaux, O. Gröning, in *Encyclopedia of Nanoscience and Nanotechnology*, vol. 1, ed. by H.S. Nalwa (American Scientific Publishers, 2004), p. 547
4. A.G. Rinzler, J.H. Hafner, P. Nikolaev, L. Lou, S.G. Kim, D. Tomanek, P. Nordlander, D.T. Colbert, R.E. Smalley, Science **269**, 1550 (1995)
5. W.A. de Heer, A. Châtelain, D. Ugarte, Science **270**, 1179 (1995)
6. P.G. Collins, A. Zettl, Phys. Rev. B **55**, 9391 (1997)
7. J.M. Bonard, F. Maier, T. Stoeckli, A. Chatelain, W.A. de Heer, J.P. Salvetat, L. Forro, Ultramicroscopy **73**, 7 (1998)
8. S. Fan, M.G. Chapline, N.R. Franklin, T.W. Tombler, A.M. Cassell, H. Dai, Science **283**, 512 (1999)
9. Y. Saito, S. Uemura, Carbon **38**, 169 (2000)
10. O. Groning, O.M. Kuttel, Ch. Emmenegger, P. Groning, L. Schlapbach, J. Vac. Sci. Technol. B **18**(2), 665 (2000)
11. L. Nilsson, O. Groening, C. Emmenegger, O. Kuettel, E. Schaller, L. Schlapbach, H. Kind, J.M. Bonard, K. Kern, Appl. Phys. Lett. **76**, 2071 (2000)
12. M. Chhowalla, C. Ducati, N.L. Rupesinghe, K.B.K. Teo, G.A.J. Amaratunga, Appl. Phys. Lett. **79**, 2079 (2001)
13. J.S. Suh, K.S. Jeong, S. Lee, I. Han, Appl. Phys. Lett. **80**, 2392 (2002)
14. K.B.K. Teo, M. Chhowalla, G.A.J. Amaratunga, W.I. Milne, G. Pirio, P. Legagneux, F. Wyczisk, D. Pribat, D.G. Hasko, Appl. Phys. Lett. **80**, 2011 (2002)
15. S.H. Jo, Y. Tu, Z.P. Huang, D.L. Carnahan, D.Z. Wang, Z.F. Ren, Appl. Phys. Lett. **82**, 3520 (2003)
16. R.B. Rakhi, K. Sethupathi, S. Ramaprabhu, Nanoscale Res. Lett. **2**, 331 (2007)
17. J.-M. Bonard, J.-P. Salvetat, T. Stockli, W.A. de Heer, L. Forro, A. Châtelain, Appl. Phys. Lett. **73**, 918 (1998)
18. W. Zhu, C. Bower, O. Zhou, G. Kochanski, S. Jin, Appl. Phys. Lett. **75**, 873 (1999)
19. C.H. Weng, K.C. Leou, H.W. Wei, Z.Y. Juang, M.T. Wei, C.H. Tung, C.H. Tsai, Appl. Phys. Lett. **85**, 4732 (2004)
20. Sk.F. Ahmad, S. Das, M.K. Mitra, K.K. Chattopadhyay, Appl. Surf. Sci. **254**, 610 (2007)
21. V.I. Merkulov, A.V. Melechko, M.A. Guillorn, D.H. Lowndes, M.L. Simpson, Chem. Phys. Lett. **350**, 381 (2001)
22. C.L. Tsai, C.F. Chen, L.K. Wu, Appl. Phys. Lett. **81**, 721 (2002)
23. S.K. Srivastava, A.K. Shukla, V.D. Vankar, V. Kumar, Thin Solid Films **492**, 124 (2005)
24. Y. Wu, B. Yang, B. Zong, H. Sun, Z. Shen, Y. Feng, J. Mater. Chem. **14**, 469 (2004)
25. C.J. Huang, Y.K. Chih, J. Hwang, A.P. Lee, C.S. Kou, J. Appl. Phys. **94**, 67 (2003)
26. L.-H. Chen, J.F. AuBuchon, A. Gapin, C. Daraio, P. Bandaru, S. Jin, D.W. Kim, I.K. Yoo, C.M. Wang, Appl. Phys. Lett. **85**, 5373 (2004)
27. C.J. Huang, C.M. Yeh, M.Y. Chen, J. Hwang, C.S. Kou, J. Electrochem. Soc. **153**(1), H15–H17 (2006)
28. X. Sun, R. Li, B. Stansfield, J.-P. Dodelet, G. Mènard, S. Dèsilets, Carbon **45**, 732 (2007)
29. S.K. Srivastava, V.D. Vankar, V. Kumar, Thin Solid Films **515**, 1552 (2006)
30. X. Ma, E.G. Wang, Appl. Phys. Lett. **78**, 978 (2001)
31. J.W. Jang, C.E. Lee, S.C. Lyu, T.J. Lee, C.J. Lee, Appl. Phys. Lett. **84**, 2877 (2004)
32. S.K. Srivastava, D.V. Sridhar Rao, V.D. Vankar, V. Kumar, Thin Solid Films **515**, 1851 (2006)
33. S. Hofmann, M. Cantoro, B. Kleinsorge, C. Casiraghi, A. Parvez, J. Robertson, C. Ducati, J. Appl. Phys. **98**, 034308 (2005)
34. R.T.K. Baker, Carbon. **27**, 315 (1989)
35. K.B.K. Teo, D.B. Hash, R.G. Lacerda, N.L. Rupeshinghe, M.S. Bell, S.H. Dalal, D. Bose, T.R. Govindan, B.A. Cruden, M. Chhowalla, G.A.J. Amaratunga, M. Meyyappan, W.I. Milne, Nano Lett. **5**, 921 (2004)
36. P.E. Nolan, D.C. Lynch, A.H. Cutler, J. Phys. Chem. B **102**, 4165 (1998)
37. L. Delzeit, I. McAninch, B.A. Cruden, D. Hash, B. Chen, J. Han, M. Meyyappan, J. Appl. Phys. **91**, 9027 (2002)
38. Z. Xu, X.D. Bai, E.G. Wang, Z.L. Wang, Appl. Phys. Lett. **87**, 163106 (2005)
39. J. Robertson, J. Vac. Sci. Technol. B **17**, 659 (1999)
40. C.Y. Zhi, X.D. Bai, E.G. Wang, Appl. Phys. Lett. **81**, 1690 (2002)
41. Z.P. Huang, Y. Tu, D.L. Carnahan, Z.F. Ren, in *Encyclopedia of Nanoscience and Nanotechnology*, vol. 1, ed. by H.S. Nalwa (American Scientific Publishers, 2004), p. 401
42. Y. Chen, D.T. Shaw, L. Guo, Appl. Phys. Lett. **76**, 2469 (2000)
43. R. Sen, B.C. Satishkumar, A. Govindaraj, K.R. Harikumar, G. Rainja, J.P. Zhang, A.K. Cheetham, C.N.R. Rao, Chem. Phys. Lett. **287**, 671 (1998)